

Medical Image Processing using a SIMD Array Processor and Neural Networks

Himadri Nath Moulick, Moumita Ghosh

ABSTRACT: *An SIMD parallel implementation of Kass et al's "snake" algorithm is reported, and demonstrated in use for interpreting medical images. The SIMD machine acts as a "compute server" to a generalpurpose AI environment, which provides and interactive user interface, or controls the server autonomously. This paper reviews the application of artificial neural networks in medical image preprocessing, in medical image object detection and recognition. Main advantages and drawbacks of artificial neural networks were discussed. By this survey, the paper try to answer what the major strengths and weakness of applying neural networks for medical image processing would be.*

Keywords: *Neural Network; Medical Image preprocessing; Object Detection; Computer Aided Diagnosis.*

I. Introduction

This paper reports work carried out within the BIOLAB consortium of the CEC Advanced Informatics in Medicine(AIM) programme. The overall purpose of the work is to assess the potential for commercially available parallel computer systems to enhance practical applications of medical image analysis. Here, we report methods developed for using the Active Memory Technology (AMT) DAP as a "compute server" to a network of workstations. We report three technical developments. • A parallel implementation of the "snake" algorithm of Kass, Witkin&Terzopoulos, extended to deal with closed contours ("bubbles"). • A software interface between a development environment on the remote SUN workstations and the DAP, providing either autonomous or interactive control of the "bubbles". • A demonstration of the use of the DAP as a more conventional "compute server" to the workstations, giving access to a set of conventional low-level algorithms, forming part of the AMT image processing library. The configuration is intended to assess the opportunities for using specialised parallel computers within a network of biomedical workstations. The DAP acts as a remote-access engine giving considerably improved performance over a single workstation in the network. The workstation displays the images to the user and provides an interactive interface, allowing high-level control of the system. The DAP facilities have been integrated within the Interactive Vision Environment (IVE, initially developed under Alvey grant MMI-007), which runs within the AI development environment POPLOG. The numerical computing power of the DAP is thereby coupled to the general-purpose reasoning power only available in serial machines. The benefits and costs of the SIMD machines such as the DAP in this context are examined and reported. In the past years, artificial neural networks (ANNs) have seen an increasingly interests in medical image processing[1]-[2]. According to our searching results with Google Scholar, more than 33000 items were found on the topic of medical image processing with ANNs during the past 16 years. The intention of this article is to cover those approaches introduced and to make a map for ANN techniques used for medical image processing. Instead of trying to cover all the issues and research aspects of ANNs in medical image processing, we focus our discussion on three major topics: medical image pre-processing, medical image segmentation, and medical image object detection and recognition. We do not contemplate to go into details of particular algorithms or describe results of comparative experiments, rather we want to summarize main approaches and point out interesting parts of the neural networks for medical image processing, further more by this survey, we try to answer what the major strengths and weaknesses of applying ANNs for medical image processing would be.

II. APPLICATIONS OF NEURAL NETWORKS IN MEDICAL IMAGE PROCESSING

Pre-processing

Image pre-processing with neural networks generally falls into one of the following two categories: image reconstruction and image restoration. The Hopfield neural network is one of the most used neural works for image reconstruction [3]-[7]. Of our reviewed literatures related to this area, Hopfield neural network based methods pose 55 percent. The major advantage of using Hopfield neural network for medical image reconstruction is that the problem of medical image reconstruction can be taken as an optimization problem, which is easily solved by letting the network converge to a stable state while minimizing the energy function. Reconstruction of images in electrical

impedance tomography requires the solution of a nonlinear inverse on noisy data. This problem is typically ill-conditioned and requires either simplifying assumptions or regularization based on a priori knowledge. The feed forward neural network [8]-[9] and the self-organizing Kohonen neural network [10]-[11], which pose 2 of 9 papers among our reviewed literatures, respectively, seem to have more advantage for such medical image reconstruction compared with other techniques, they can calculate a linear approximation of the inverse problem directly from finite element simulations of the forward problem. The majority of applications of neural networks in medical image pre-processing are found in medical image restoration, 13 of 24 papers among our reviewed literatures focused their interests here [12]-[21]. Among which, one paper for Hopfield neural network, seven papers for the feed forward neural network, and two papers for fuzzy neural network and for cellular neural network, respectively. In the most basic medical image restoration approach, noise is removed from an image by filtering. Suzuki et al. developed neural network based filters (NFs) for this problem [12]-[14]. Suzuki et al. Also proposed a new neural edge enhancer (NEE) based on a modified multilayer neural network, for enhancing the desired edges clearly from noisy images [15]. The NEE is a supervised edge enhancer: Through training with a set of input noisy images and teaching edges, the NEE acquires the function of a desired edge enhancer. Compared with conventional edge enhancers, the NEE was robust against noise, was able to enhance continuous edges from noisy images, and was superior to the conventional edge enhancers in similarity to the desired edges.

B. Image segmentation

The feed forward neural network is the most used neural network for medical image segmentation. Among our reviewed papers, 6 of 17 papers employed the feed forward network for medical image segmentation [22]-[27]. Compared with the traditional Maximum Likelihood Classifier (MLC) based image segmentation method, it has been observed that the feed forward neural network based segmented images appear less noisy, and the feed forward neural network classifier is also less sensitive to the selection of the training sets than the MLC. However, most feed forward neural network based methods have a very slow convergence rate and require a priori learning parameters. These drawbacks limited the application of feed forward neural networks in medical image segmentation. Hopfield neural networks were introduced as a tool for finding satisfactory solutions to complex optimization problems. This makes them an interesting alternative to traditional optimization algorithms for medical image reconstruction which can be formulated as optimization problem. Among our reviewed literatures, 4 of 17 papers used Hopfield neural network to segment some organs from a medical image [28]-[31].

C. Object detection and recognition

For using neural networks for medical image detection and recognition, the back propagation neural network poses most places, 11 of 23 papers among our reviewed literatures employed it [37]-[47]. Compared with conventional image recognition methods, no matter used for the interpretation of mammograms [37], or used for cold lesion detection in SPECT image [38], or used for diagnosing classes of liver diseases based on ultrasonographic [39], or used for separation of melanoma from three benign categories of tumors [41], or distinguish interstitial lung diseases [42], or used for reduction of false positives in computerized detection of lung nodules in LDCT [43]-[46] and chest radiography [47], all these feed forward neural network based methods show their preference in recognition accuracy and computing time compared with conventional methods. Other neural networks, i.e. Hopfield neural network [48], ART neural network [49], radial basis function neural network [50], Probabilistic Neural Network [51], convolution neural network [53]-[56], and fuzzy neural network [52] [57], have also found their position in medical image detection and recognition, which poses 1 of 23, 1 of 23, 1 of 23, 1 of 23, 2 of 23 and 2 of 23 papers, respectively. Different from what mentioned above, in [58] and [59], artificial neural network ensembles are employed for cancer detection. The ensemble is built on two-level ensemble architecture. The first-level ensemble is used to judge whether a cell is normal with high confidence where each individual network has only two outputs respectively normal cell or cancer cell. The predictions of those individual networks are combined by some method. The second-level ensemble is used to deal with the cells that are judged as cancer cells by the first-level ensemble, where each individual network has several outputs respectively, each of which represents a different type of lung cancer cells. The predictions of those individual networks are combined by a prevailing method, i.e. plurality voting. Experiments show that the neural network ensemble can achieve not only a high rate of overall identification but also a low rate of false negative identification, i.e. a low rate of judging cancer cells to be normal ones, which is important in saving lives due to reducing missing diagnoses of cancer patients.

III. THE AMT-DAP 510: OVERVIEW

The DAP is a commercially available array processor, whose basic design has not changed since the 1970s. It represents a cost-effective way of increasing raw computing power for some applications. The DAP 510 processor consists of an array of 32 by 32 processor elements (PEs), connected in a fixed square grid (AMT, 1988). Each PE is a 1-bit computer, running at a clock rate of 10MHz. This gives each processor about the power of a PC or a SUN 3, but all arithmetic is carried out bit-serial, so the realisable performance greatly depends on the algorithms employed. All PEs carries out instructions under the control of a single program. Each PE has 4Kbytes of local memory which is also used to store the images. There is no general shared memory. The DAP has a hi-resolution, colour graphics monitor, served by a frame-buffer that can be read or written in parallel by the PEs. The DAP is interfaced to a host SUN 3/50, by means of a SCCSI port, which carries all communications between the DAP and the host (and hence the SUN network). The DAP is normally programmed in an extended form of Fortran which allows automatic use of vector and matrix parallelism. A library of standard control software on the host can be called from either Fortran or C. This includes software for passing data to and from the DAP, loading, starting and interrupting the DAP, and for passing SUN mouse information to the DAP.

A. Implementation

The DAP510 comprises an array of 32x32 processors. We therefore define each bubble as one or more sequences of 32 control points, each point being assigned to one processor. The full array is then able to compute 32 sequences inparallel, which can be assigned to arbitrary combinations of bubbles each having multiples of 32 points (e.g. 32 x 32-point bubbles, 4 x 256-point bubbles, 1 x 1024-point bubble etc). The positions of each control point is advanced stepwise in time, and each timestep comprises three phases. During the first or FORCE phase, the local gradient of the image is found at each control point. This requires random access to the 512x512 byte image, stored amongst the PEs. This is achieved by a tightly coded scalar loop in APAL assembler code. In the next or MOVE phase, the net force at a point is computed from the local image force, internal forces due to the positions of its neighbours (tension and stiffness), and the internal pressure term. The equations of motion are:

$$\frac{dx}{dt} = \frac{d}{ds} \left(T \frac{dx}{ds} \right) - S \frac{d^2 x}{ds^2} + P_x - \frac{dI}{dx}$$

$$\frac{dy}{dt} = \frac{d}{ds} \left(T \frac{dy}{ds} \right) - S \frac{d^2 y}{ds^2} + P_y - \frac{dI}{dy}$$

In these equations, s is a parametric variable advancing by unity between successive control points. The first term on the RHS gives the effect of an elastic string with an elastic constant T , which acts as a variable tension in the string proportional to the separation between bubble points. With this term alone, the exact solution between two fixed points is a straight line with equidistant bubble points, as one would expect for an elastic string. The second term on the RHS provides the bubble with stiffness determined by the value of s , and a tendency to resist sharp changes of curvature. The third term is a constant internal pressure force which acts along the line joining the centre of gravity of the bubble points to the surface bubble point in question. In order to prevent the pressure force from translating the bubble in the absence of an image, the average value of the pressure force over all the bubble points is made zero. The last term is the gradient of the image intensity I , or the image force term previous calculated in the FORCE phase. The solution of the equations of motion is obtained by finite differencing, and stability for any sized timestep is ensured by using an implicit differencing scheme (see[1]for details). This leads to a five-diagonal set of equations for the new positions of each bubble, that is to say the need to solve 32 five-diagonal sets of equations, first for x then for y . The parallel solution is obtained using the method of cyclic reduction, actually an extension to a five-diagonal matrix of the PARACR algorithm described in reference [2]. Finally, the last or GRAPHICS phase of the timestep uses the directly connected DAP display monitor to plot the new positions of all snake points on the image. Having found all the new bubble positions in parallel, the timestep is repeated continuously, and the bubbles relax towards positions tending to lie along the bubble-shaped objects in the image. However, even when the points are stationary, the DAP is continuously computing them; that is to say the bubbles are 'alive' at all times, and will respond instantly if any points are interactively moved.

B. Control of Shape and Size

In the absence of an image, the steady state solution to the above bubble equations with periodic (or cyclic) boundary conditions in the s -variable, and constant values for tension and stiffness, is a circle. If the stiffness is zero then the radius of the circle is proportional to the ratio of pressure to tension, just as it would be for a soap bubble.

The introduction of stiffness slightly decreases the radius of the circle. The pressure can therefore be conveniently used to vary the size of the bubble in a natural way. If the tension is varied around the bubble surface (i.e. as a function of the variable s), then the shape of the bubble can be varied. Different harmonic functions may be applied to the elastic tension and summed. In principle this provides a simple means for defining a wide range of closed, convex shapes. Limited experiments have been carried out using the second and third harmonics, Massing the bubble towards given elliptical or ovoidal shapes.

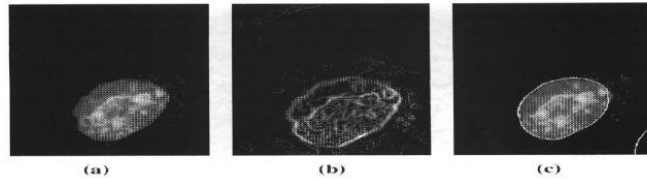


Fig 1. A single 32 node bubble interacting with an isolated cell (a) original image, (b) modulus of the smoothed gradient, (c) the bubble overlaid on (a).

C. Examples

Fig1 demonstrates a simple interaction between a 32- point bubble and an image of an isolated cell. The image, Fig1(a), was first smoothed by a 2-D gaussian distribution ($a = 1$ pixel), and an image corresponding to the modulus of the discrete gradient vector was computed, Fig 1(b). A small bubble was placed inside the cell in Fig1(b). Under the influence of the pressure term, the bubble grew, until it was caught and held by the image maxima. When stable, the bubble's position outlines the cell boundary fairly accurately - Fig 1(c). The time to stabilise depends on the match between the initial shape parameters of the bubble, and the image distribution. It is strongly affected by the time-step used in the algorithm. A large time-step causes the bubble to respond rapidly to the forces on it, but this can lead to instability and oscillation. In the examples shown here, the convergence time (for each bubble) was approximately 2-4 seconds. Better convergence schemes, based on simulated annealing methods can improve performance (see below). The power of the parallel implementation of bubbles is more evident in images consisting of multiple cells. Fig 2 shows 32 bubbles interacting with an edge-differentiated cell image. The centres of suspected cells were first identified by finding peaks in a smoothed Laplacian image (where the scale of the smoothing is adjusted to suit the expected cell size.). Bubbles were then placed in the image at these points. In most cases the bubbles have adjusted their shape to that of the actual cells and have become attached to them. The settling time for all 32 bubbles is again about 2 seconds.

D. Performance

The performance of the AMT DAP relative to a typical workstation was measured by having the host computer perform the same calculation at the same time as the DAP. Timings were obtained individually for the different phases of the timestep for both the DAP and the SUN, and the overall speedup ratio of the calculation was calculated. Timings given below refer to the SUN 3/50 host machine.

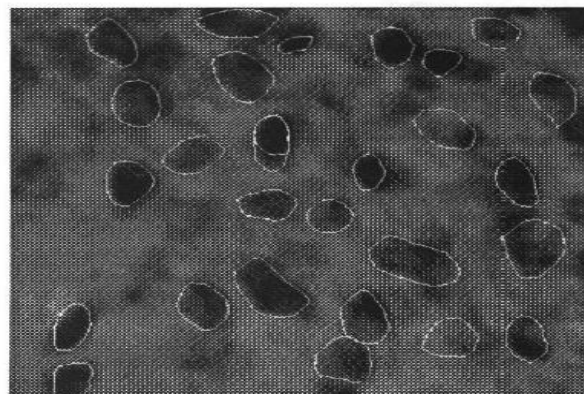


Fig 2 .1J bubble parallel placed automatically in

PROCESSING PHASE	Times in msec		Speed-up Ratio
	SUN 3/50	DAP510	
FORCE	2639	70	37
MOVE	1020	18	56
GRAPHICS	4000	95	41
TIMESTEP	7659	183	41

These timings show that on the DAP only 10% of the time is spent solving the motion equations - the bulk of the time is consumed in the FORCE calculations and the GRAPHICS output. The FORCE phase is dominated by the essentially serial random image access routines, using carefully coded assembler routines in APAL which picks up one byte from the image at a time.



Fig 3. showing two bubbles, interacting with the scalp outline and the cortical surface

Comparisons using a SUN 4/20 indicate that (as expected), the SUN 4 performs about 10 times as fast as the SUN3. This gives a speed-up advantage for the DAP of merely 4. However, when used in the networked configuration (see below) the graphics phases and the control parameter processing of the DAP program can be dropped. This restores the advantage to about a factor of 10. It should be noted that the DAP-510 has fairly low processing power: a larger DAP can be configured with 64*64 PEs, and a faster machine, with 8-bit arithmetic is scheduled. In this work the DAP is used to represent SIMD compute servers; the bubble algorithm could easily be adapted to other, faster SIMD machines. More modern machines have mechanisms for shared memory, with indirect addressing in the PEs, which would greatly speed up the calculations in the FORCE phase of the program.

IV. CONTROL MECHANISMS

Bubbles can only act to refine the localisation of structure in the image, since they must initially be placed close enough to an appropriate attractor. Unguided, they merely fall into arbitrary local minima. One potential practical role for deformable models in medical image processing applications is to provide an "intelligent" tool to assist the clinician in making interactive measurements of image features, and our initial DAP deformable model algorithm was developed for such direct use.

A. Work station control

The DAP graphics screen only allows single-user access. At present, such under-use of an array processor cannot be

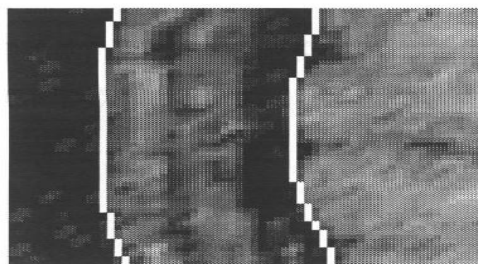


Fig 4. Close-up view of part of Fig3., showing two bubbles, interacting with the scalp outline and the cortical surface justified on cost grounds. Medical image processing applications typically occur intermittently. It is therefore attractive to seek to network the DAP as a "compute server" for many workstations. This has the additional advantage that the GRAPHICS part of the algorithm can be delegated to the workstation, thus increasing the performance by about a factor of 2 (see table). The DAP-SUN SCCSI link gives the host computer full control of the DAP. The DAP program repeatedly checks the host SUN for messages, requesting a read or write of either the

system parameters or the position of the control points. This allows a program written on the host machine to control the compute engine. To provide for user interaction with the program on the SUN workstations, we have developed a simple link between the DAP and POPLOG running on SUN 3 or 4 (or other) machines within the network. Within POPLOG, the DAP engine has been integrated into a vision systems development tool developed and used extensively in house (the Interactive Vision Environment - IVE). Fig 3 shows a screen dump from a typical session. This facility allows the DAP programs to be used on a singleuserbasis across the network. Multiple users are managed by the existing multi-tasking operating system of the DAP. In a dedicated system, a remote demon is envisaged to improve the efficiency of time sharing between multiple workstations.

V. DISCUSSION

We have described a SIMD implementation of the algorithms reported by Kass, Witkin and Terzopoulos. The use of the parallel computer makes new methods for interactive image processing feasible. Such processing is likely to be of particular importance in the domain of medical image processing, where the clinician often needs to control the analysis of an image by hand, yet would greatly welcome increased assistance from the computer in outlining important structures. Much time is currently spent in radiological laboratories to identify structures in images manually, to identify regions which require further processing. The example shown in Fig 1 is of a cell from a cervical smear: the degree of irregularity in the boundary of the cell is a primary indicator of a pre-cancerous condition. The cells in Fig 2 have been stained by means of mono-clonal antibodies which attach to the active sites involved in rheumatoid arthritis; the type of staining, and the size and shape of the stained cells are of importance for contemporary research into the causes and treatment of rheumatism. Active deformable models can form a variety of structures. The smooth, closed "bubbles" described here have particular use in cytological applications, but other structures are currently being investigated. Fig 4 shows the outline scalp extracted from MR slice images. Each slice was pre-filtered to create an image of the modulus of the gradient. A bubble was placed near the edge of the image, outside the head region, with low pressure. It rapidly shrank and was trapped onto the outer gradient peak. The elastic term was then reduced, so that the position of the bubble was dominated by the image data. Fig 3 and 4 were captured during this operation. The cortical boundary has also been approximated in these images by a second bubble, half the size of the first bubble, placed inside the scalp and then expanded by increasing the pressure. This reliably avoids many of the artifacts associated with the use of edge maps, as reported in Attwood et al (1990). In principle it should be possible to process multiple slices simultaneously, though software to do this is still under development. This would allow 32 slices such as are shown in Fig 4 to be computed in parallel, and outlines similar to these to be computed in a few seconds. The further use of DAP graphics routines for viewing and shading the results are also intended. Two other extensions of this work are of special interest: (i) The use of higher order terms in the definition of the shape of the bubble. Bubbles are biased by the harmonics in the elasticity, and by the choice of starting conditions. It is therefore possible to model more complex structures, such as the ventricles of the heart in cine-angiography, or organs of the brain in cranial radiography. These models can be stored in a database of anatomical shapes, called up according to the clinical context, (ii) Methods for forming 2-D rubber sheets, in a 32*32 array. Many medical imaging methods produce series of slices such as in Figure 4, which capture the 3-D structure of organs being imaged. It is straightforward to extend the ID snakes (moving in a 2D image) to 2D membranes (moving in 3D data). This will provide the ability to "shrink-wrap" 3D structures directly, rather than building them from independently processed slices.

VI. CONCLUSION

From the reviewed literatures, we find that no matter what neural network model employed for medical image processing, compared with conventional image processing methods, the time for applying a trained neural network to solve a medical image processing problem was negligibly small, though the training of a neural network is a time cost work and also medical image processing tasks often require quite complex computation [12]-[15]. We think that this may be the major contribution of using neural network for solving medical image processing tasks. Despite their success story in medical image processing, artificial neural networks have several major disadvantages compared to other techniques. The first one is that a neural network is hard to express human expert's knowledge and experience, and the construction of its topological structure lacks of theoretical methods [60]. Moreover the physical meaning of its joint weight is not clear. All these can make the image processing method by neural networks unstable. A solution to these problems may be to combine fuzzy technique with neural networks together by using neural networks to process fuzzy information. It provides neural networks the ability to express qualitative knowledge, and network topological structure and joint weight have clear physical meaning. Also, it can make the initialization of network easier, avoid the local optimization of network training, and ensure the stability of

networks [61]. The second problem relates to the amount of input data. For achieving a high and reliable performance for non-training cases, a large number of training cases are commonly required [62] [63]. If an ANN is trained with only a small number of cases, the generalization ability (performance for non-training cases) will be lower (e.g., the ANN may fit only the training cases). Because medical images are progressing rapidly as technology advances, the timely development of CAD schemes is important. However, it is very difficult to collect a large number of abnormal cases for training, particularly for a CAD scheme with a new modality, such as lung cancer screening with multi-detector-row CT. This significantly degraded the results obtained. The very high speed implementation on a parallel machine makes the techniques of deformable models feasible for clinical and research applications. The speed-up achieved transforms algorithms for deformable models from a computational curiosity, to one which would appear to have immediate practical significance. This implementation is based on an SIMD machine, available commercially for the cost of a typical mini-computer. This order of cost can be justified in a networked, multi-tasking system.

REFERENCES

- [1] Kunio Doi, "Computer-Aided Diagnosis in Medical Imaging: Historical Review, Current Status and Future Potential," *Computerized Medical Imaging and Graphics*. vol.31, no.4-5, pp.198-211, July 2007.
- [2] Miller A.S, Blott B.H, Hames T.K. , "Review of Neural Network Applications in Medical Imaging and Signal Processing," *Medical and Biological Engineering and Computing*. vol.30, no.5, pp.449-464, September 1992.
- [3] A. Cichocki, R. Unbehauen, M. Lendl, K. Weinzierl, "Neural Networks for Linear Inverse Problems with Incomplete Data Especially in Applications to Signal and Image Reconstruction," *Neurocomputing*. vol.8, no.1, pp.7-41, May 1995.
- [4] W. Warsito, L.S. Fan, "Neural Network Based Multi-Criterion Optimization Image Reconstruction Technique for Imaging Two and Three Phase Flow Systems Using Electrical Capacitance Tomography," *Chemical Engineering and Processing*. Vol.42, no.8-9, pp.2198-2210, April 2001.
- [5] B. Su, Y. Zhang, L. Peng, D. Yao, B. Zhang, "the Use of Simultaneous iterative reconstruction technique for electrical capacitance tomography," *Chemical Engineering Journal*. Vol.77, no.1-2, pp.37-41, April 2000.
- [6] Y. Wang, F.M. Wahl, "Vector-Entropy Optimization-Based Neural-Network Approach to Image Reconstruction from Projections," *IEEE Trans. Neural Networks*. Vol.8, no.5, pp.1008-1014, September 1997.
- [7] Y. Wang, P. Heng, F.M. Wahl, "Image Reconstructions from Two Orthogonal Projections," *International Journal of Imaging Systems and Technology*. vol.13, no.2, pp.141-145, Aug. 2003.
- [8] F. Ali, Z. Nakao, Y.-W. Chen, K. Matsuo, I. Ohkawa, "An Adaptive Backpropagation Algorithm for Limited-Angle CT Image Reconstruction," *IEICE Trans. Fundamentals*. Vol.E83-A, no.6, pp.1049-1058, 2000.
- [9] A. Netajatali, I.R. Ciric, "An Iterative Algorithm for Electrical Impedance Imaging Using Neural Networks," *IEEE Trans. Magn.* Vol.34, no.5, pp.2940-2943, September 1998.
- [10] C. Comtat, C. Morel, "Approximate Reconstruction of PET Data with a Self-Organizing Neural Network," *IEEE Trans. Neural Networks*. Vol.6, no.3, pp.783-789, May 1995.
- [11] A. Adler, R. Guardo, "A Neural Network Image Reconstruction Technique for Electrical Impedance Tomography," *IEEE Transactions on Medical Imaging*. Vol.13, no.4, pp.594-600, 1994.
- [12] Kenji Suzuki, Isao Horiba, Noboru Sugie and Michio Nanki, "Neural Filter with Selection of Input Features and Its Application to Image Quality Improvement of Medical Image Sequences," *IEICE Transaction on Information and Systems*. Vol.E85, no.10, pp.1710-1718, 2002.
- [13] K. Suzuki, I. Horiba, and N. Sugie, "A Simple Neural Network Pruning Algorithm with Application to Filter Synthesis," *Neural Process. Lett.* Vol.11, no.1, pp.45-53, February 2001.
- [14] K. Suzuki et al, "Efficient Approximation of Neural Filters for Removing Quantum Noise from Images," *IEEE Trans. Signal Process.* vol.50, no.7, pp.1787-1799, July 2002.
- [15] K. Suzuki et al, "Neural Edge Enhancer for Supervised Edge Enhancement from Noisy Images," *IEEE Trans. Pattern Anal. Mach. Intell.* Vol.25, no.12, pp.1582-1596, December 2003.
- [16] Chuan Yu Chang, "Contextual-Based Hopfield Neural Network for Medical Image Edge Detection," *Optical Engineering*. Vol.45, pp.37006-37015, March 2006.
- [17] Clarke, L.P., Wei Qian, "Fuzzy Logic Adaptive Neural Networks for Nuclear Medicine Image Restorations," *Proceedings of the 20th Annual International Conference of the IEEE*. Vol.3, pp.1363-1366, July 1998.
- [18] Qian W., Li H., Kallergi M., Song D., Clarke L. P., "Adaptive Neural Network for Nuclear Medicine Image Restoration," *The Journal of VLSI Signal Processing*. Vol.18, no.3, pp.297-315, April 1998.
- [19] N. Aizenberg, I. Aizenberg, T.P. Belikova, "Extraction and Localization of Important Features in Gray-Scale Images: Implementation with CNNs," *Proceedings of the IEEE International Workshop on Cellular Neural Networks and their Applications CNNA, Rome, Italy, IEEECS Press, Silver Springs*, pp.207-212, December 1994.
- [20] I. Aizenberg, "Processing of Noisy and Small-Detailed Gray-Scale Images Using Cellular Neural Networks," *Journal of Electronic Imaging*. vol.6, no.3, pp.272-285, July 1997.
- [21] I. Aizenberg, "Multi-Valued Non-linear Filters and Their Implementation on Cellular Neural Networks," *Frontiers in Artificial Intelligence and Applications*. Vol.41, pp.135-140, 1997.
- [22] Du Yih TSAI, "Automatic Segmentation of Liver Structure in CT Images Using a Neural Network," *IEICE TRANSACTIONS on Fundamentals of Electronics, Communications and Computer Sciences*. Vol. E77-A, no.11, pp.1892-1895, November 1994.
- [23] A. Hasegawa, S.C.B. Lo, J.S. Lin, M.T. Freedman and S.K. Mun, "A Shift-Invariant Neural Network for the Lung Field Segmentation in Chest Radiography," *The Journal of VLSI Signal Processing*. Vol. 18, no. 3, pp.241-250, April 1998.

- [24] Mehmed Ozkan, Benoit M. Dawant and Robert Margolin, "Neural- Network-Based Segmentation of Multi-Modal Medical Images: A Comparative and Prospective Study," IEEE Transactions on Medical Imaging. Vol.12, no.3, pp.534-544, September 1993.
- [25] Yan Li Peng Wen Powers, D. Clark, C.R., "LSB Neural Network Based Segmentation of MR Brain Images," Systems, Man, and Cybernetics. Vol.6, pp.822-825, 1999.
- [26] Ian Middleton and Robert I. Dampier, "Segmentation of Magnetic Resonance Images Using a Combination of Neural Networks and Active Contour Models," Medical Engineering & Physics. Vol.26, no.1, pp.71-86, January 2004.
- [27] Chiou GI, Hwang JN, "A Neural Network-Based Stochastic Active Model (NNS-SNAKE) for Contour Finding of Distinct Features," IEEE Trans Image Process. Vol.4, no.10, pp.1407-1416, October 1995.
- [28] John E. Koss, F.D. Newman FD, T.K. Johnson, and D.L. Kirch, "Abdominal Organ Segmentation Using Texture Transforms and a Hopfield Neural Network," IEEE Transactions on Medical Imaging. vol.18, no.7, pp.640-648, July 1999.
- [29] Jzau-Sheng Lin, Kuo-Sheng Cheng, Chi-Wu Mao, "A Fuzzy Hopfield Neural Network for Medical Image Segmentation," IEEE Transactions on Nuclear Science. Vol.43, no.4, pp.2389-2398, August 1996.
- [30] Chwen Liang Chang and Yu Tai Ching, "Fuzzy Hopfield Neural Network with Fixed Weight for Medical Image Segmentation," Optical Engineering. Vol.41, no.2, pp.351-358, 2002.
- [31] K. S. Cheng, J.S. Lin, C.W. Mao, "the Application of Competitive Hopfield neural network to Medical Image Segmentation," IEEE Transactions on Medical Imaging. Vol.15, no.4, pp.560-567, August 1996.
- [32] Wei Sun and Yaonan Wang, "Segmentation Method of MRI Using Fuzzy Gaussian Basis Neural Network," Neural Information Processing. Vol.8, no.2, pp.19-24, August 2005.
- [33] Chien-Cheng Lee, and Pau-Choo Chung, "Recognizing Abdominal Organs in CT Images Using Contextual Neural Networks and Fuzzy Rules," In Proc. of Int. Conf. of the IEEE Engineering in Medicine and Biology Society, pp. 1745-1748, Chicago, IL, July 23-28 2000.
- [34] Y. Wang, T. Adali, S.Y. Kung et al, "Quantification and Segmentation of Brain Tissues from MR Images - a Probabilistic Neural Network Approach," IEEE Transactions on Image Processing. Vol.7, no.8, pp.1165-1181, August 1998.
- [35] W. E. Reddick, J.O. Glass, E.N. Cook et al, "Automated Segmentation and Classification of Multispectral Magnetic Resonance Images of Brain Using Artificial Neural Networks," IEEE Trans. Med. Imaging. Vol.16, no.6, pp.911-918, December 1997.
- [36] A. Pitiot, A.W. Toga, N. Ayache, P. Thompson, "Texture Based MRI Segmentation with a Two-Stage Hybrid Neural Classifier," Proceedings of the 2002 International Joint Conference on Neural Networks. vol.3, pp.2053-2058, 12-17 May 2002.
- [37] Wu Y, Giger ML, Doi K et al, "Artificial Neural Network in Mammography: Application to Decision Making in the Diagnosis of Breast Cancer," Radiology. Vol.187, pp.81-87, April 1993.
- [38] Tourassi GD, Floyd CE Jr, "Artificial Neural Networks for Single Photon Emission Computed Tomography," Invest Radiol. Vol.28, no.8, pp.671-677, August 1993.
- [39] Maclin PS, Dempsey J, "Using Artificial Neural Networks to Diagnose Hepatic Masses," Journal of Medical Systems. Vol.16, no.5, pp.215-225, October 1992.
- [40] Wolberg WH, Sreet WN, Mangasarian OL, "Image Analysis and Machine Learning Applied to Breast Cancer Diagnosis and Prognosis," Anal Quant Cytol Histol. Vol.17, no.2, pp.77-87, April 1995.
- [41] Fikret Ercal, Anurag Chawla, William V. Stoecker, His-Chieh Lee, and Randy H. Moss, "Neural Network Diagnosis of Malignant Melanoma from Color Images," IEEE Transactions on biomedical engineering. Vol.41, no.9, pp.837-845, September 1994.
- [42] Ashizawa K, Ishida T, MacMahon H, Vyborny CJ, Katsuragawa S, Doi K, "Artificial Neural Networks in Chest Radiography: Application to the Differential Diagnosis of Interstitial Lung Disease," Academic Radiology. Vol.6, no.1, pp.2-9, January 1999.
- [43] K. Suzuki, S. G. Armato, F. Li, S. Sone, and K. Doi, "Massive Training Artificial Neural Network (MTANN) for Reduction of False Positives in Computerized Detection of Lung Nodules in Low-Dose CT," Med. Phys. Vol.30, no.7, pp.1602-1617, July 2003.
- [44] K. Suzuki, S. G. Armato, F. Li, S. Sone, and K. Doi, "Effect of a Small Number of Training Cases on the Performance of Massive Training Artificial Neural Network (MTANN) for Reduction of False Positives in Computerized Detection of Lung Nodules in Low-Dose CT," In Proc. SPIE (Medical Imaging). Vol.5023, pp.1355-1366, July 2003.
- [45] K. Suzuki and K. Doi, "Characteristics of a Massive Training Artificial Neural Network (MTANN) in the Distinction Between Lung Nodules and Vessels in CT Images," in Computer Assisted Radiology and Surgery (CARS), Chicago, IL, pp.923-928, 2004.
- [46] H. Arimura, S. Katsuragawa, K. Suzuki, F. Li, J. Shiraishi, S. Sone, and K. Doi, "Computerized Scheme for Automated Detection of Lung Nodules in Low-Dose CT Images for Lung Cancer Screening," Acad. Radiol. Vol.11, no.6, pp.617-629, June 2004.
- [47] K. Suzuki, J. Shiraishi, H. Abe, H. MacMahon, and K. Doi, "False-Positive Reduction in Computer-Aided Diagnostic Scheme for Detecting Nodules in Chest Radiographs by Means of Massive Training Artificial Neural Network," Acad. Radiol. Vol.12, no.2, pp.191-201, February 2005.
- [48] Zhu Y, Yan H, "Computerized Tumor Boundary Detection Using a Hopfield Neural Network," IEEE Transactions on Medical Imaging. Vol.16, no.1, pp.55-67, February 1997.
- [49] Innocent PR, Barnes M, John R, "Application of the Fuzzy ART/MAP and MinMax/MAP Neural Network Models to Radiographic Image Classification," Artif. Intell. in Med. Vol.11, no.3, pp.241-263, 1997.
- [50] Yasser M. Kadah, Aly A. Farag, Jacek M. Zaruda, Ahmed M. Badawi, and Abou-Bakr M. Youssef, "Classification Algorithms for Quantitative Tissue Characterization of Diffuse Liver Disease from Ultrasound Images," IEEE transactions on Medical Imaging. Vol.15, no.4, pp.466-478, August 1996.
- [51] E-Liang Chen, Pau-Choo Chung, Ching-Liang Chen, Hong-Ming Tsai and Chein I Chang, "An Automatic Diagnostic system for CT Liver Image Classification," IEEE Transactions Biomedical Engineering. Vol.45, no.6, pp.783-794, June 1998.
- [52] Pavlopoulos S, Kyriacou E, Koutsouris D, Blekas K, Stafylopatis A, Zoumpoulis P, "Fuzzy Neural Network-Based Texture Analysis of Ultrasonic Images," IEEE Engineering in Medicine and Biology. Vol.19, no.1, pp.39-47, Jan-Feb. 2000.
- [53] H. P. Chan, S.C.B. Lo, B. Sahiner et al, "Computer-Aided Detection of Mammographic Microcalcifications: Pattern Recognition with an Artificial Neural Network," Medical Physics vol. 22, no.10, pp.1555-1567, October 1995.
- [54] B. Sahiner, H.P. Chan, N. Petrick et al, "Classification of Mass and Normal Breast Tissue - a Convolution Neural Network Classifier with Spatial Domain and Texture Images," IEEE Transactions on Medical Imaging. Vol.15, no.5, pp.598-610, October 1996.
- [55] S. C. B. Lo, H.P. Chan, J.S. Lin et al, "Artificial Convolution Neural Network for Medical Image Pattern Recognition," Neural Networks. Vol.8, no.7-8, pp.1201-1214, 1995.
- [56] H P Chan et al, "Computerized Classification of Malignant and Benign Microcalcifications on Mammograms: Texture Analysis Using an Artificial Neural Network," Phys. Med. Biol. Vol.42, no.3, pp.549-567, March 1997.

- [57] B. Verma, J. Zakos, "A Computer-Aided Diagnosis System for Digital Mammograms Based on Fuzzy-Neural and Feature Extraction Techniques," *IEEE Transactions on Information Technology in Biomedicine*. Vol.5, no.1, pp.46-54, March 2001.
- [58] ZhiHua Zhou, Yuan Jiang, Yu Bin Yang, Shi Fu Chen, "Lung Cancer Cell Identification Based on Artificial Neural Network Ensembles," *Artificial Intelligence in Medicine*. Vol.24, no.1, pp.25-36, January 2002.
- [59] K. Tumer, N.Ramanujam, J. Ghosh, and R. Richards-Kortum, "Ensembles of Radial Basis Function Networks for Spectroscopic detection of Cervical Precancer," *IEEE Transactions on Biomedical*. Vol.45, no.8, pp.953-961, August 1998.
- [60] L. Perlovsky, "Conundrum of combinatorial complexity," *IEEE Transactions on Pattern Analysis and Machine Intelligence*. Vol.20, no.6, pp.666-670, June 1998.
- [61] AMT Technical Overview: The AMT DAP 500. 1988
- [62] Attwood, CI, Sullivan GD, Robinson, G., Baker KD and Colchester ACF. BMVC90, 1990 (These Proceedings)
- [63] Burr, D.J. Elastic Matching of Line Drawings. *IEEE PAMI*-3,6, 708-713 (1981)
- [64] Hockney R W and Jesshope C R, "Parallel Computers 2", Adam Hilger/IOPP, Bristol and New York (1988) 479-483. Distributed in USA by American Institute of Physics, NY.
- [65] Kass M, Witkin A, Terzopoulos D, "Snakes: Active Contour Models", *IEEE Proc. First ICCV* (1987) 259-268
- [66] Mowforth, P.H and Zhengping, J. Model-based tissue Differentiation. *Proceedings of the AVC89*, 67-73(1989).